Optimization of breastshot water wheels performance using different inflow configurations

Optimization of breastshot water wheels performance using different inflow configurations

Quaranta E.*, Revelli R.**

Politecnico di Torino, DIATI (Department of Environment, Land and Infrastructure Engineering). Corso Duca degli Abruzzi 24, 10129, Torino, Italia

Abstract

Breastshot water wheels are gravity hydraulic machines employed in low head sites. The scope of this work is to test the performance of a breastshot water wheel with two geometric inflow configurations: a sluice gate at different openings and two vertical overflow weirs. With the sluice gate, the maximum efficiency of the plant is 75%, constant over a wide range of flow rates, while the efficiency with the weir is increasing in the same flow rate range. Therefore, the wheel with the weir can exploit higher water volumes, and also it performs better at high power input. In practical applications, the inflow configuration can be effectively controlled to optimize the operative working conditions of breastshot water wheels, depending on the external hydraulic ones. The experimental results are also discussed in dimensionless terms, in order to support engineers in the design of similar breastshot water wheels.

*(corresponding author). E-mail: emanuele.quaranta@polito.it, quarantaemanuele@yahoo.it
**E-mail: roberto.revelli@polito.it

Keywords: micro-hydro; overflow weir; sluice gate; water mills; water wheels.

1. Introduction

The wheel has been one of the most ancient technology used by mankind to produce energy. The first vertical water wheel was the *stream* water wheel, still used nowadays in flowing water [1]. The water interacts with the blades below the wheel and the kinetic energy of streams drives the wheel. In *gravity* wheels (*overshot*, *breastshot* and *undershot* water wheels) the weight of water is mainly employed for the generation of energy, in sites where a geometric head difference exists (the difference of the channel's bed elevation upstream and downstream of the wheel). In overshot water wheels the water enters into the cells from the top of the wheel. They are generally used for head differences between 2.5 and 10 m and at low flow rates (approximately from 0.2 to 1.0 m^3/s per unit width). In breastshot wheels the water enters into the buckets near the rotation axle. These wheels are usually employed for head differences lower than 4 m and at flow rates from 0.5 to 2.0 m^3/s per unit width. When the geometric head difference is very low (e.g. $1/8 \div 1/10$ of the diameter, although there not exists a precise limit), breastshot water wheels can be called *low* breastshot wheels, or undershot wheels: the water fills the buckets in the lowest part of the wheel and these wheels are generally used at flow rates from 1 to 3 m^3/s per unit width.

During the Eighteenth and Nineteenth century, some experimental tests and theoretical estimations for the determination of the efficiency of water wheels were developed [2] [3] [4] [5] [6] [7] [8]. However, the previous studies generally were not totally satisfactory, since theoretical analyses were not supported by experimental tests, and comparisons among different geometric configurations under the same hydraulic conditions were generally not presented. Therefore,

the most of the available engineering and scientific information is ancient, with uncertainty and often published in not well known text-books.

At the beginning of the Twentieth century, the rising demand of energy, the economic development and the rapid improvement in the engineering knowledge (especially the design of big hydroelectric plants and the transmission of electricity), led to the introduction and diffusion of modern turbines, employed in big hydroelectric plants with heads of tens/hundreds meters. Therefore, the classical water wheels, used in low head sites especially for self sustainment, were replaced and by then considered ancient and bygone machines.

In the last years, due to their numerous purposes, quite high efficiency, low payback periods, low environmental impact and simplicity of construction [9], water wheels are regarded again as interesting hydraulic machines for the production of decentralized energy, especially when combined with a mill for grinding wheat. Indeed, it is a general view that bread made by water mill's flour is tastier than that produced by electric engines and it has also a finer quality and higher nutritive value [10]. When installed in old water mills, water wheels may also contribute to the preservation of the cultural heritage, the development of tourism, the promotion of local manufacture and the creation of employment. Hence water wheels may become a profitable industry, especially due to the wide diffusion on the territory of sites suitable for water wheels [11]. These machines may be also an interesting investment in rural areas, since their payback periods are low ($7 \div 14$ years with respect to 30 years for a Kaplan installation) [9].

Therefore, thanks to the previous motivations, the interest of the scientific community in water wheels is starting to increase. For example, recent scientific studies on undershot and stream wheels can be found in [1] [12] [13] [14] [15].

In [16] a study of an overshot water wheel is presented. Concerning breastshot water wheels, in [17] [18] theoretical and dimensional analysis, respectively, have been performed for a breastshot wheel equipped with a sluice gate.

2. Breastshot water wheels

Since this work will investigate different inflow configurations of a breastshot water wheel, it is worthwhile to cite the book of *Garuffa* [7], where breastshot water wheels are classified as *fast* and *slow*. Figure 1 shows a *fast* breastshot wheel, where the inflow configuration is constituted of a sluice gate. Figure 2 depicts a *slow* breastshot water wheel, where the inflow configuration is constituted of an overflow weir. In this book, the previous terminology is inspired by the fact that in fast breastshot wheels the flow accelerates passing under the sluice gate. The flow velocity to the wheel is hence faster with respect to the flow velocity in *slow* wheels, where the water passes over an overflow weir just upstream of the wheel, entering into the buckets from higher elevations. This means that, considering the same flow rate, head difference and wheel rotational speed, the torque contribution of the water weight in *slow* wheels is higher with respect to the torque contribution of the water weight in *fast* breastshot wheels. In *slow* breastshot wheels the torque due to the kinetic energy of water is lower with respect to *fast* wheels.

Although it is not mandatory to install one of the previous hydraulic structures upstream of a water wheel, they are useful. These inflow structures allow to regulate and to optimize the operative working conditions. Sluice gates and weirs are usually present in irrigation canals, where suitable conditions for breastshot water wheels exist. Due to the higher flow velocity, in fast breastshot wheels the

kinetic energy of the flow can contribute significantly to the driving torque of the wheel. In order to exploit efficiently the kinetic energy of the flow, the inclination of the blades surface has to be parallel to the flow relative velocity ($\vec{w}$) at the entry point, as shown in Fig. 1. The relative velocity is defined as the vector difference between the absolute entry velocity of water ($\vec{v}$) and the tangential velocity of the wheel ($\vec{u}$). The opening (a) of the sluice gate can be regulated to control the absolute velocity of the flow to the wheel, hence the relative velocity.

No complete and detailed experimental comparisons on the performance of slow and fast breastshot wheels have been found in modern literature, under the same hydraulic conditions. Therefore, in order to shed light on this issue, the aim of the present paper is to perform experimental tests on a breastshot water wheel, investigating its performance with an inflow weir and a sluice gate. In practical operative conditions, the inflow configuration can be managed depending on the external hydraulic conditions, optimizing the efficiency of the hydro plant. Scope of the present paper is thus to determine in which conditions it is more advisable to use the weir, and when it is better to regulate the flow to the wheel acting on the opening of the sluice gate.

3. Method

3.1. Experimental equipment and procedure

An experimental channel has been installed in the Laboratory of Hydraulics at Politecnico di Torino with the aim of testing different kinds of water wheels; in this work the results of a breastshot water wheel are presented. The diameter of the wheel was D=2R=2.12 m, the width was b=0.65 m and the number of the blades was 32 (Fig. 3).

The flow rate Q to the wheel was set acting on a pump and a gate valve installed in the supply pipe of the channel (flow rates $Q = 0.02 \div 0.1$ m^3/s were investigated). The flow rate was detected by an electromagnetic flow meter, whose accuracy was $\delta Q = \pm 0.5 \cdot 10^{-3}$ m^3/s. A brake system, constituted of a generator and a resistor, was connected at the wheel's shaft. An electrical energy analyzer and a control of the electrical resistance were installed to manage the electrical power output of the generator and the load on the wheel, regulating the rotational speed N of the wheel ($N = 0.2 \div 2.1$ rad/s). The minimum rotational speed depended on the maximum braking torque that the brake could apply. The maximum rotational speed was close to the runaway velocity. Between the wheel and the brake, a gearbox was installed to provide an optimum speed and torque range on the generator shaft. Along the shaft an inductive proximity sensor was installed in order to acquire the rotational speed of the wheel. A torque transducer was also installed along the transmission shaft to measure the shaft torque (C_{exp}) with a precision of $\delta C_{exp} = \pm 6$ Nm. The experimental power output $P_{exp} = C_{exp} \cdot N$ was determined by multiplying the applied torque C_{exp} by the rotational speed N. The rotational speed was measured by the internal clock of the acquisition board, which could discretize the output signal frequency of the proximity sensor till 100 MHz, with very high accuracy.

In order to evaluate the power input to the wheel, the upstream and downstream water depths, h_u and h_d, respectively, were measured, obtaining the head difference, or difference of energy head:

$$H_{gr} = (H_U - H_D) = \left[\left(z_u + h_u + \frac{{v_u}^2}{2g} \right) - \left(z_d + h_d + \frac{{v_d}^2}{2g} \right) \right] \qquad (1)$$

where H_U is the energy head upstream of the wheel (measured 2.5 m from the axle of the wheel), H_D the downstream one (energy head at the tailrace, 0.89 m from the axle of the wheel) and $H_{gr} = H_U - H_D$ is the head difference. The energy head H_x is the sum of the channel's bed elevation z_x, the water depth h_x and the kinetic term ${v_x}^2/2g$, where $g = 9.81$ m/s^2 is the acceleration of gravity and v_x is the mean flow velocity (Fig.4). The mean flow velocity is calculated as $v_u = Q/l_u h_u$ and $v_d = Q/l_d h_d$, where $l_u = 1.5$ m and $l_d = 0.67$ m are the widths of the channel in the measurement points. In our case, the geometric head difference is $H_g = z_u - z_d = 0.35$ m, thus the ratio $r = H_g/D = 0.165$. The water depth h_u was monitored by an ultrasonic sensor with a precision of $\delta h_u = \pm 0.004$ m and the downstream depth h_d by a classical ruler, with the operator precision of $\delta h_d \simeq 0.002$ m. While the upstream water depth depended on the opening of the sluice gate or the height of the inflow weir, the downstream water depth was not regulated by any hydraulic structure.

The power input of the hydroelectric plant was:

$$P_{gr} = \rho g Q H_{gr} \tag{2}$$

where Q is the total flow rate and $\rho = 1000$ Kg/m^3 is the density of water.

The global efficiency of the installed hydroelectric plant is defined as η:

$$\eta = \frac{P_{exp}}{P_{gr}} \tag{3}$$

and it is a function of the flow rate, rotational speed and inflow configuration.

3.1.1. ***Error analysis***

Scope of this section is to apply the error propagation laws to estimate the error δ on each quantity derived from the experimental measurements.

The width of the channel b, the wheel radius R and the geometric head H_g are considered known, thus without error.

As written in the previous section, the error of the measurements is $\delta h_u = \pm 0.004$ m for the upstream water depth, $\delta h_d = \pm 0.002$ m for the downstream one, $\delta Q = \pm 0.5 \cdot 10^{-3}$ m^3/s for the flow rate and $\delta C_{exp} = \pm 6$ Nm for the torque.

The estimated error of the power output can be calculated as:

$$\delta P_{exp} = \pm P_{exp} \cdot \frac{\delta C_{exp}}{C_{exp}} = \pm 6 \cdot N \tag{4}$$

since the rotational speed was calculated with very high accuracy.

Considering that the generic velocity is $v_x = Q/(bh_x)$, the error of the velocity measurement can be calculated as:

$$\frac{\delta v_x}{v_x} = \frac{\delta Q}{Q} + \frac{\delta h_x}{h_x} \tag{5}$$

where the subscript x can refer both to the upstream quantities (flow velocity v_u and water depth h_u), and to the downstream ones (v_d and h_d). The error of the velocity to the second power (the kinetic term) is:

$$\frac{\delta {v_x}^2}{{v_x}^2} = 2\frac{\delta v_x}{v_x} \rightarrow \delta {v_x}^2 = 2 v_x \delta v_x \tag{6}$$

where δv_x can be calculated by eq.5.

The error of the head difference (eq.1) estimation can be calculated as:

$$\delta H_{gr} = \delta h_u + \frac{1}{2g}\delta {v_u}^2 + \delta h_d + \frac{1}{2g}\delta {v_d}^2 \tag{7}$$

where $\delta {v_x}^2 = 2{v_x}^2 \left(\frac{\delta Q}{Q} + \frac{\delta h_x}{h_x}\right)$.

The error of the measurement of the power input $P_{gr} = \rho g Q H_{gr}$ can be quantified in:

$$\delta P_{gr} = \rho g(\delta[QH_{gr}]) = \rho g Q H_{gr} \left(\frac{\delta Q}{Q} + \frac{\delta H_{gr}}{H_{gr}}\right) \tag{8}$$

Finally, the error of the efficiency estimation ($\eta = P_{exp}/P_{gr}$) can be expressed as:

$$\delta \eta = \eta \left(\frac{\delta P_{exp}}{P_{exp}} + \frac{\delta P_{gr}}{P_{gr}}\right) \tag{9}$$

3.2. Inflow geometric configurations

The first experiments dealt with the breastshot wheel equipped with a sluice gate, as illustrated in Fig. 4. In the figure, by the point E we identify the water entry point to the wheel. The sluice gate was installed 0.7 m upstream of point E and its opening was varied between $0.050 < a < 0.150$ m. The opening of the sluice gate allowed to regulate the upstream water depth h_u, thus the flow velocity to the wheel. Therefore, while the flow velocity was often negligible upstream of the sluice gate (especially at small sluice gate openings), it was not negligible when the flow entered into the wheel, because of the flow acceleration passing under the sluice gate. The total number of experiments was: 39 for the sluice gate opening $a = 0.05$ m, 53 for $a = 0.075$ m, 59 for $a = 0.100$ m, 55 for $a = 0.125$ m, 48 for $a = 0.150$ m. During experiments, first of all the flow rate was set by the

pump, then the sluice gate adjusted to the requested opening and, at the end, the rotational speed was regulated by the brake.

After the first set of experiments, the sluice gate was removed, and the channel was equipped with a vertical weir (as illustrated in Fig. 5), changing the water entry point to the wheel. Weirs of 0.18 m and 0.28 m high were investigated. The advantage of a vertical weir is its simplicity and facility of regulation. Each weir was located just before the wheel, in order to ensure a gap of about 0.01 m between the top edge of the weir and the blades, as illustrated in Fig. 5, in order to avoid any contact between the wheel and the weir. The weir 0.18 m high was installed 0.12 m upstream of the water entry point (E in Fig. 5), and the weir 0.28 m high was installed 0.17 m upstream of the entry point. The flow rate was then set by the pump and the rotational speed of the wheel regulated by the brake.

In this case, the weir was a vertical wall, thus its downstream profile did not fit the circular shape of the wheel (the circular path of the blade tip during its rotation). This led to volumetric losses (see Fig. 5): a portion of water flows from the buckets toward the space V. Anyway, the water which is initially lost from the bucket is not definitively lost, since it re-enters into the buckets (the losses are not so high, since a portion of the volume V is filled of water). In order to contain the volumetric losses (consider that the higher the weir, the more distant it has to be installed from the wheel), the height of the weir should be $< 1 \div 1.5$ times the depth of the buckets (the external distance between two blades). This recommendation justifies the investigated heights; considering the diameter of the wheel of 2.12 m and 32 blades, the depth of the buckets is about 0.2 m.

A total of 42 and 36 experiments for the configurations with the weir of height $h_s = 0.18$ m and $h_s = 0.28$ m, respectively, were carried out. When the weir was in operation, the water flow did not accelerate passing under the sluice gate and it entered into the wheel from higher elevation and at lower velocity. Therefore, considering a certain flow rate, the torque contribution of the water weight increases with the weir, whereas the torque contribution due to the kinetic energy of the flow reduces.

4. Results and discussion

4.1. Experimental results and discussion

Scope of the present section is to compare the performance of the breastshot water wheel in the two inflow configurations. During experiments, the flow rate was firstly imposed. When the sluice gate was in operation, the entry flow velocity was regulated acting on the opening of the sluice gate and the rotational speed of the wheel regulated by means of the brake. Instead, when the weir was in operation, only the flow rate and the wheel rotational speed needed to be regulated. Consider a representative case with $Q = 0.05$ m^3/s, $h_u = 0.5$ m, $h_d = 0.1$ m (hence $H_{gr} = 0.72$ m and $P_{gr} = 354$ W), $N = 1$ rad/s, and $\eta = 0.7$ (hence $P_{exp} = 248$ W). The accuracy of the head difference estimation is $\delta H_{gr} = 0.0078$ m, $\delta P_{gr} = 7.35$ W for the power input, $\delta P_{exp} = 6$ W for the power output and $\delta\eta = 0.031$ for the efficiency. These values are lower if compared to their respective measured quantities, hence they can be considered acceptable.

Figure 6 depicts some efficiency curves for selected flow rates. In the weir configuration the efficiency trend is quite constant, while in the sluice gate configuration the efficiency increases up to a maximum, and then it decreases (the

maximum power output occurs in correspondence of the maximum efficiency). This difference can be explained in this way. The kinetic energy of the flow entering into the wheel is lower when the weir is installed with respect to the kinetic energy of the flow when the sluice gate is installed (the flow accelerates passing under the sluice gate). Hence the contribution of the kinetic energy of the flow to the torque (as well as to the efficiency) is lower in the weir configuration. Since the wheel rotational speed affects especially the transfer of kinetic energy from the flow to the wheel (i.e. the relative flow velocity and the impact power losses), it is reasonable that the efficiency trend is less affected by the wheel velocity when the weir is installed.

For each flow rate, the height of the weir affects the efficiency not significantly, while the opening of the sluice gate is very important. The lower the opening, thus the higher the water velocity to the wheel, the lower the efficiency. The efficiency reduction with the lowering of the sluice gate is worsened with the increase of the flow rate, since the water velocity also increases with the flow rate. High water velocities generate significant power losses both during the filling process due to the impact, and in the conveying channel [17]. One other aspect that can be observed for the sluice gate is that the higher the flow rate, the higher the optimal rotational speed (the speed at maximum efficiency). This occurs for the following motivation. As it will be illustrated in section 4.2, the optimal rotational speed is proportional to the square root of the head difference. The higher the flow rate, the higher the upstream water depth, thus the higher the required rotational speed for the optimal efficiency. This can also be justified by the fact that the higher the upstream water depth, the faster the flow velocity to the wheel, thus the higher the value that the rotational speed can assume to

optimize the impact conditions.

Figure 7 shows the maximum experimental power output versus the flow rate. For the cases with the sluice gate, the power output increases with the reduction in the sluice gate opening, due to the higher entry flow velocity. When the weir is in operation, the power output increases with the height of the weir, due to the increase in the elevation of the water entry point, thus in the potential energy of water. The maximum power output for the weir configuration is usually higher at a certain flow rate. This occurs because when the weir is installed, the water weight begins to push the blades from higher elevations, although the torque due to the kinetic energy of the flow is lower, with respect to what happens with the sluice gate. Since the weir leads to higher power output, this means that the increase in the torque due to the water weight is more important than the decrease in the kinetic contribution. However, at flow rates bigger than 0.08 m^3/s the trend of the power output for sluice gate openings lower than 0.075 m seems to overcome the trend for the cases with the weir.

Figure 8a depicts the efficiency versus the flow rate. The first general result that can be seen is the difference between the efficiency trends of the wheel in the two geometric inflow configurations. Considering the cases with the sluice gate, the efficiency increases up to a maximum value. Then, for $a > 0.10$ m the maximum value is also almost constant at 75%; the range of constant efficiency is included between $Q = 0.05$ to $Q = 0.08 \div 0.09$ m^3/s. This range corresponds to $(0.56 \div 0.6) \cdot Q_{max}$ and Q_{max}, where Q_{max} is the maximum flow rate in the range of constant efficiency for each geometric inflow configuration. For sluice gate openings ≤ 0.10 m there is not a constant efficiency range, and Q_{max} corresponds to the flow rate at the maximum efficiency. The efficiency starts to decrease from

$Q = 0.05 \div 0.06$ m^3/s. The smaller the sluice gate opening, the lower Q_{max}. This is justified by the fact that at a certain flow rate, the smaller the opening of the sluice gate, the higher the upstream water depth and the water velocity to the wheel, thus the more significant the power losses upstream of the wheel. Therefore, the smaller the sluice gate opening, the lower the allowable flow rate in order to avoid excessive flow velocity to the wheel and power losses.

Instead, considering the inflow weirs, the efficiency trend is increasing and more regular (Fig.8a). This result says that the optimal flow rate is higher in the weir configuration (due to the geometric limitations of the experimental channel, it was not possible to investigate higher flow rates). Hence the configuration with the weir allows to exploit efficiently larger flow volumes, i.e. flow rates $Q > 0.08$ m^3/s in the present case. The efficiency of the plant equipped with the weir is also higher at very low discharges. The maximum efficiency at flow rates of $Q = 0.02$ m^3/s improves from $\eta = 0.25 \div 0.30$ with the sluice gate to $\eta = 0.45$ using the weir. This occurs because at very low flow rates the contribution of the kinetic energy is negligible; therefore, it is more convenient to use a weir in order to enhance the water elevation, instead of exploiting the kinetic energy by reducing the sluice gate opening.

The previous considerations show that the efficiency with the sluice gate exhibits a stronger dependence from the flow rate. This result is confirmed in [19], where a breastshot water wheel equipped with an inflow weir has been investigated: its efficiency was constant already from flow rates of $0.2 \cdot Q_{max}$, while the present breastshot wheel with the sluice gate has constant efficiency in the range $(0.56 \div 0.6) \cdot Q_{max}$ and Q_{max}.

In Fig.8b it can be observed that in the range $P_{gr} = 150 \div 400$ W the ef-

ficiency with the weir is lower, probably due to the volumetric losses occurring downstream of the weir, as explained in section 3.2, while the efficiency is higher for $P_{gr} > 400$ W. The efficiency at high power inputs ($P_{gr} > 400$ W) decreases with the reduction of the sluice gate opening. This occurs because such situation corresponds to high flow rates and upstream water depths h_u, leading to high flow velocities downstream of the sluice gate, and, as a consequence, significant power losses in the impact against the blades and in the headrace, due to friction and turbulence [17]. Hence the use of the weir becomes more advisable than the sluice gate in these conditions.

A comparison between the two inflow weirs shows that the power output of the highest weir is generally higher than the power output of the shortest weir (Fig. 7), whereas the efficiencies are similar (Fig. 8).

4.2. Practical applications and discussion

As discussed in the previous section, the paper has showed that the optimal hydraulic conditions where the inflow weir and the sluice gate should operate are different. In particular, the weir works better in extreme conditions, that is for low and high flow rates and power inputs. Therefore, the combination and the regulation of the sluice gate and the weir can be considered a suitable method to optimize the working conditions and the efficiency of breastshot water wheels.

The regulation of the sluice gate opening can be also a way to control the operational speed of the wheel, when the flow rate is not constant, in order to guarantee always the optimal operative conditions for the constant speed of operation. When the flow rate changes, also the optimal speed of the wheel changes, since the optimal rotational speed depends on the flow rate. In order to shed

light on this, Fig.9 depicts the rotational speed at the maximum efficiency versus the sluice gate opening at different flow rates, for the tested wheel. Therefore, at a fixed sluice gate opening and flow rate, the wheel rotational speed required to obtain the maximum efficiency is determined. For each flow rate, the trend is nearly linear: the lower sluice gate openings (a) (thus the higher the flow velocity to the wheel), the higher the wheel rotational speed required to obtain the maximum efficiency (as discussed for Fig.6). As a consequence, when it is desirable that the wheel operates at a constant rotational speed also with variable flow rates, using a graph similar to Fig.9, it is possible to determine for each flow rate the sluice gate opening which guarantees that the same rotational speed remains optimal. Furthermore, since the graph is drawn using the maximum efficiency data, the optimal operative conditions are also guaranteed. The control of the sluice gate can cooperate with the weir, to be used at very low and big flow rates. Otherwise, if the variable speed of operation is allowed, and the geometric configuration is fixed (fixed sluice gate opening in this case), a control system must be able to change the wheel rotational speed, depending on the flow rate. However, a variable speed of operation requires a costly rectifier/control/inverter system, and expensive gearboxes [9]. Therefore, since the constant speed is more advisable, the sluice gate opening can be regulated to change the hydraulic configuration and to guarantee that the rotational speed (which is constant) continue to be optimal also at variable flow rates.

Some results are now discussed as a function of dimensionless parameters, making the performance results generically applicable. First of all, in a practical application the diameter can be chosen in order to obtain a geometrically similar water wheel, hence ensuring the same value of $r_p = H_{g,p}/D_p = 0.165$, where with

the subscript p we refer to the variables in the practical case (the wheel at full scale). It is then possible to determine the optimal inflow configuration, wheel rotational speed and width, as explained in the following lines.

The optimal inflow configuration can be estimated by Fig. 10, which shows the maximum efficiency versus the normalized power input. The normalized power input is defined as follows [18]:

$$P_{gr}^{*} = \frac{P_{gr} \cdot {H_g}^4}{\rho Q^3} \tag{10}$$

whose error (considering the representative case, to which corresponds $P_{gr}^{*} = 42.5$) can be estimated as:

$$\delta P_{gr}^{*} = \frac{{H_g}^4}{\rho} \delta \left[\frac{P_{gr}}{Q^3} \right] \rightarrow \frac{{H_g}^4}{\rho} \frac{P_{gr}}{Q^3} \left(\frac{\delta P_{gr}}{P_{gr}} + 3 \frac{\delta Q}{Q} \cdot Q^3 \right) = 0.88 \tag{11}$$

Figure 10 can be used to determine the optimal inflow condition as a function of the normalized power input (in order to ensure the maximum efficiency). The normalized power input depends on the full scale geometric head difference and on the operative flow rate. Since the power input depends on the inflow configuration, which is not known yet, an iterative process has to be adopted. In Fig.10, the dimensions of the inflow configurations are scaled to the geometric head difference H_g (which is 0.35 m in our case), obtaining the normalized sluice gate opening a^* and weir height ${h_s}^*$. The graph can also be used as useful generalized tool to estimate the wheel efficiency as a function of the hydraulic conditions. In Fig.10, the lower the flow rate, the higher the dimensionless power input for each configuration. Observing the trends starting from the highest power inputs, hence for increasing flow rates, the trends with the sluice gate initially increase,

reaching a maximum, which occurs at the optimal P^*_{gr}, thus the optimal flow rate. After the maximum, the trends decrease considerably for sluice gate openings $a \leq 0.10$ m or $a^* \leq 0.286$. The smaller the sluice gate opening the higher the optimal dimensionless power input at the maximum efficiency, thus the lower the optimal flow rate (as discussed in the description of Fig.8). Instead, the trends of the weir do not exhibit a maximum, because the experimental channel did not allow to explore higher flow rates. For $P^*_{gr} > 70$ it is more advisable to use the weir. For $P^*_{gr} < 70$ the efficiency trends of the weir and of the sluice gate are practically coincident, except when the efficiency trends for $a^* \leq 0.286$ decrease at normalized power input lower than the optimal.

Once the inflow configuration is determined, by Tab.1 the optimal rotational speed can be estimated. Table 1 shows the optimal normalized tangential speeds u^* of the wheel at the highest efficiency for each inflow case and flow rate ($u = NR$).

$$u^* = \frac{N \cdot R}{\sqrt{2gH_{gr}}} \tag{12}$$

whose error (for the same previous representative case to which corresponds $u^* = 0.266$) can be estimated as:

$$\delta u^* = \frac{R}{\sqrt{2g}} \frac{N}{\sqrt{H_{gr}}} \left(\frac{\delta N}{N} + \frac{1}{2} \frac{\delta H_{gr}}{H_{gr}} \right) = 0.0014 \tag{13}$$

The wheel tangential speed was normalized to the term $\sqrt{2gH_{gr}}$, in order to make the results both applicable in a general case, as also done in [15] for *Zuppinger* and *Sagebien* water wheels, and to relate the rotational speed to the hydraulic conditions.

Considering optimal flow rates $Q > 0.03$ m^3/s for the cases with the sluice gate, the normalized tangential speeds are approximately included in the range $u^* = 0.3 \div 0.4$ (which is a quite limited range). For a certain flow rate, these values are almost constant at different sluice gate openings; instead they slightly increase with the flow rate (at a constant sluice gate opening). This means that the optimal tangential speed is mainly affected by the square root of the head difference. Instead $u^* = 0.16 \div 0.4$ for the cases with the weir and the height of the weir affects noticeably u^* (remember that from Fig.6 the efficiency was not strongly affected by the wheel velocity, thus the efficiency at the optimal speed is not so higher than the efficiency at different wheel speeds). The calculated ranges are in agreement with those found for *Zuppinger* and *Sagebien* water wheels [15], which are between 0.2 and 0.4.

Table 2 reports the filling ratio of the buckets at the highest efficiency for each inflow case and flow rate. The filling ratio is defined as the ratio of the water volume inside the bucket to the bucket volume, which is delimited by two blades and the channel's bed. The optimal filling ratio is included in the range $0.3 \div 0.45$ for the sluice gate and $0.27 \div 0.6$ for the weir. In a practical application, the table can be used to determine the width of the wheel, which should ensure that the optimal filling ratio is respected. In order to use these tables, the actual flow rate and inflow type have to be scaled in Froude similarity to the conditions investigated in this work. Finally, the wheel speed and width can be adjusted to ensure a water depth in the buckets higher than the tailrace water depth, to avoid adverse hydrostatic forces.

5. Conclusions and future work

Although water wheels were forgotten in the Twentieth century, nowadays they can represent interesting hydraulic machines in very low head sites. Water wheels are efficient, cheap and exhibit low environmental impacts. In particular, breastshot water wheels are used in sites with abundant flow rates, such as in irrigation and mill channels, with heads generally less than 4 m. Some of them are located in old water mills, thus their restoration can also contribute to the preservation of the natural and cultural heritage. We can also claim that water wheels are seeing a revival, but the engineering information is not completed in detail, thus further work is needed.

In this paper, experimental results are reported to illustrate how the efficiency of a breastshot water wheel changes under different hydraulic and geometric configurations. Two different inflow configurations are investigated: the former has a sluice gate upstream of the wheel (whose opening could be regulated), the second a weir. Two weirs of different heights were installed upstream of the wheel and investigated.

The maximum efficiency for sluice gate openings > 0.075 m was $\eta = 0.75$, which was quite constant in the range between $0.05 < Q < 0.08$ m^3/s for $a > 0.10$ m, while the efficiency with the weir is increasing, suggesting that the wheel is able to exploit larger water volumes. The weirs improve the efficiency of the wheel at very low discharges ($Q < 0.03$ m^3/s), and they give also appreciable effects at high power input ($P_{gr} > 400$ W).

The optimal normalized tangential speeds are included in the range $u^* = 0.3 \div 0.4$ and $u^* = 0.16 \div 0.4$ for the cases with the sluice gate and the weir,

respectively. The optimal filling ratio is approximately included in the range $0.3 \div 0.5$. These ranges can be considered optimal operative conditions for similar breastshot water wheels.

Therefore, both the correct design of the elevation of the weir and the opening of the sluice gate can be considered a suitable method to optimize the working conditions and the efficiency of breastshot water wheels.

6. Acknowledgments

The research leading to these results has received funding from ORME (Energy optimization of traditional water wheels – Granted by Regione Piemonte via the ERDF 2007-2013 (Grant Number: #0186000275) – Partners Gatta srl, BCE srl, Rigamonti Ghisa srl, Promec Elettronica srl and Politecnico di Torino). Thanks also to Paolo Cavagnero for his help in the experimental tests.

7. Bibliography

[1] Müller, G., Denchfield, S., Marth, R., and Shelmerdine, R. Stream wheels for applications in shallow and deep water. *Proc. 32nd IAHR Congress, Venice, 32(2), 2007, 707-716.*

[2] Poncelet, J.V. *Memoria sulle ruote idrauliche a pale curve, mosse di sotto, seguita da sperienze sugli effetti meccanici di tali ruote, 1843.* Translated by Errico Dombré, published by Dalla tipografia Flautina, Napoli.

[3] Morin, A., and Morris, E. *Experiments on Water wheels Having a Vertical Axis, Called Turbines, 1843.* Published at Metz and Paris, Franklin Institute.

[4] Weisbach, J. *Principles of the mechanics of machinery and engineering, 1849.* Published by Lea and Blanchard, Philadelphia.

[5] Bach, C. *Die Wasserräder: Atlas (The water wheels: technical drawings), 1886.* Published by Konrad Wittwer Verlag, Stuttgart (in German).

[6] Chaudy, F. *Machines hydrauliques, 1896.* Bibliothèque du conducteur de travaux publics. Published by Vve. C. Dunod et P. Vicq (in French).

[7] Garuffa, E. *Macchine motrici ed operatrici a fluido, 1897.* Meccanica industriale. Published by U. Hoepli (in Italian).

[8] Church, I.P. *Hydraulic Motors, with Related Subjects, Including Centrifugal Pumps, Pipes, and Open Channels, Designed as a Text-book for Engineering Schools, 1914.* Published by J. Wiley and sons.

[9] Müller, G., and Kauppert, K. Performance characteristics of water wheels. *Journal of Hydraulic Research, 42(5), 2004, 451-460.*

[10] Vashisht, AK. Current status of the traditional watermills of the Himalayan region and the need of technical improvements for increasing their energy efficiency. *Applied Energy, 98, 2012, 307-315.*

[11] European Small Hydropower Association. *Small and Micro Hydropower Restoration Handbook, 2004.*

[12] Gotoh, M., Kowata, H., Okuyama, T., and Katayama, S. Characteristics of a current water wheel set in a rectangular channel. *Proceedings of the ASME fluids engineering division summer meeting, 2, 2001, 707-712.*

[13] Tevata, A., and Chainarong, I. The Effect of Paddle Number and Immersed Radius Ratio on Water Wheel Performance. *Energy Procedia, 9 (0), 2011, 359-365.*

[14] Paudel, S., Linton, N., Zanke, U., and N. Saenger. Experimental investigation on the effect of channel width on flexible rubber blade water wheel performance. *Renewable Energy, 52, 2013, 1-7.*

[15] Quaranta, E., and Müller, G. Zuppinger and Sagebien water wheels for very low head applications. *Journal of Hydraulic Research, under review.*

[16] Quaranta, E., and Revelli, R. Output power and power losses estimation for an overshot water wheel. *Renewable Energy, (83), 2015b, 979-987.*

[17] Quaranta, E., and Revelli, R. Performance characteristics, power losses and mechanical power estimation for a breastshot water wheel. *Energy, (87), 2015a, 315-325.*

[18] Vidali, C., Fontan, S., Quaranta, E., Cavagnero, P., and Revelli, R. Experimental and dimensional analysis of a breastshot water wheel. *Journal of Hydraulic Research, 2016, DOI:10.1080/00221686.2016.1147499.*

[19] Müller, G., and Wolter, C. The breastshot waterwheel: design and model tests. *Proceedings of the ICE-Engineering Sustainability, 157(4), 2004, 203-211.*

List of Figures

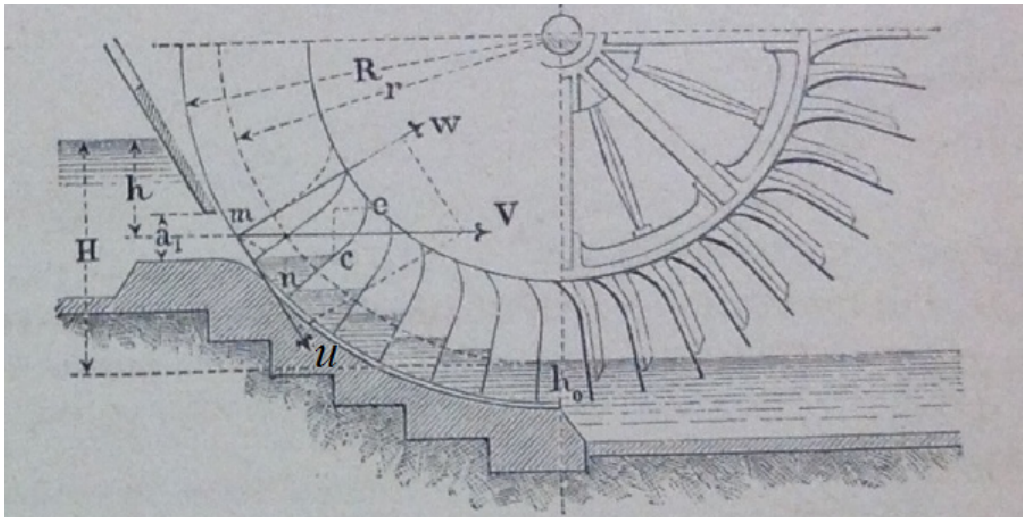

Fig. 1. Classical configuration of a fast breastshot wheel equipped with a sluice gate of opening a (Garuffa, 1897 [7]). The relative flow velocity $\vec{w} = \vec{v} - \vec{u}$ is oriented as the blades in the impact point, where $\vec{v}$ is the absolute flow velocity and $\vec{u}$ is the tangential velocity of the wheel.

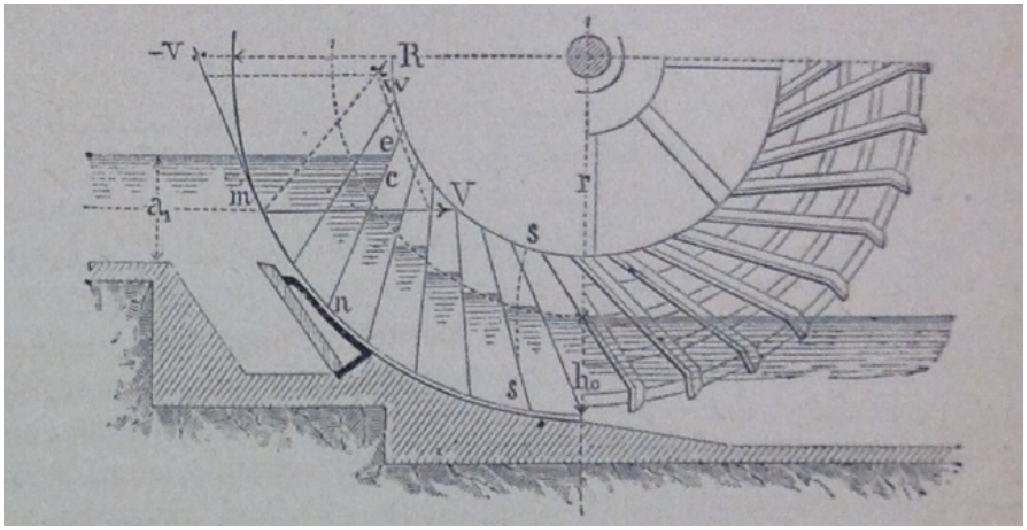

Fig. 2. Classical configuration of a slow breastshot wheel equipped with an overflow weir (Garuffa, 1897 [7]). In particular, the figure illustrates a Sagebien water wheel, that can be also considered an undershot wheel when employed in very low head applications.

Fig. 3. The installed wheel in 2.12 m in diameter and 32 blades. At the shaft axis the gearbox and the generator are visible.

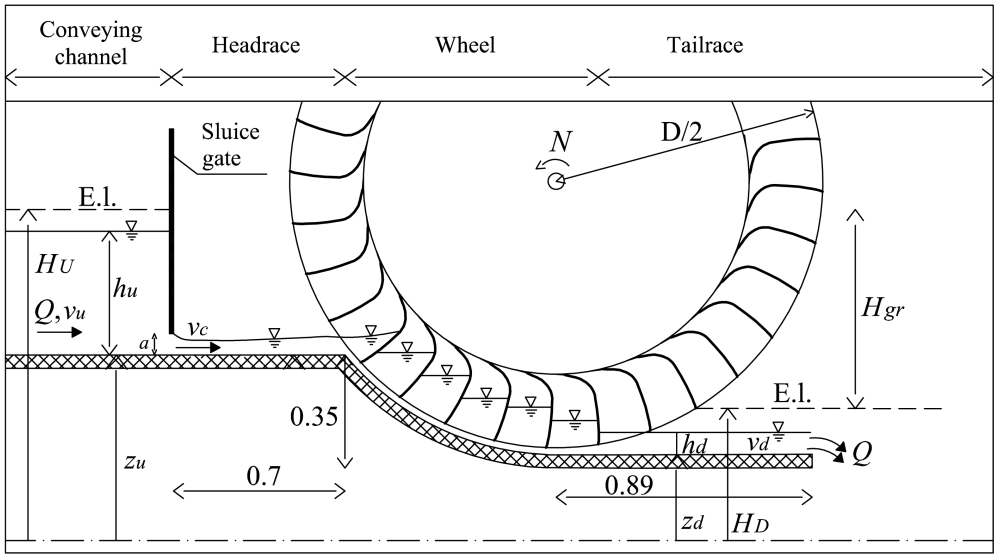

Fig. 4. The figure is the schematic representation of the investigated water wheel, with all the variables reported and some dimensions (meters). E.l. = energy line.

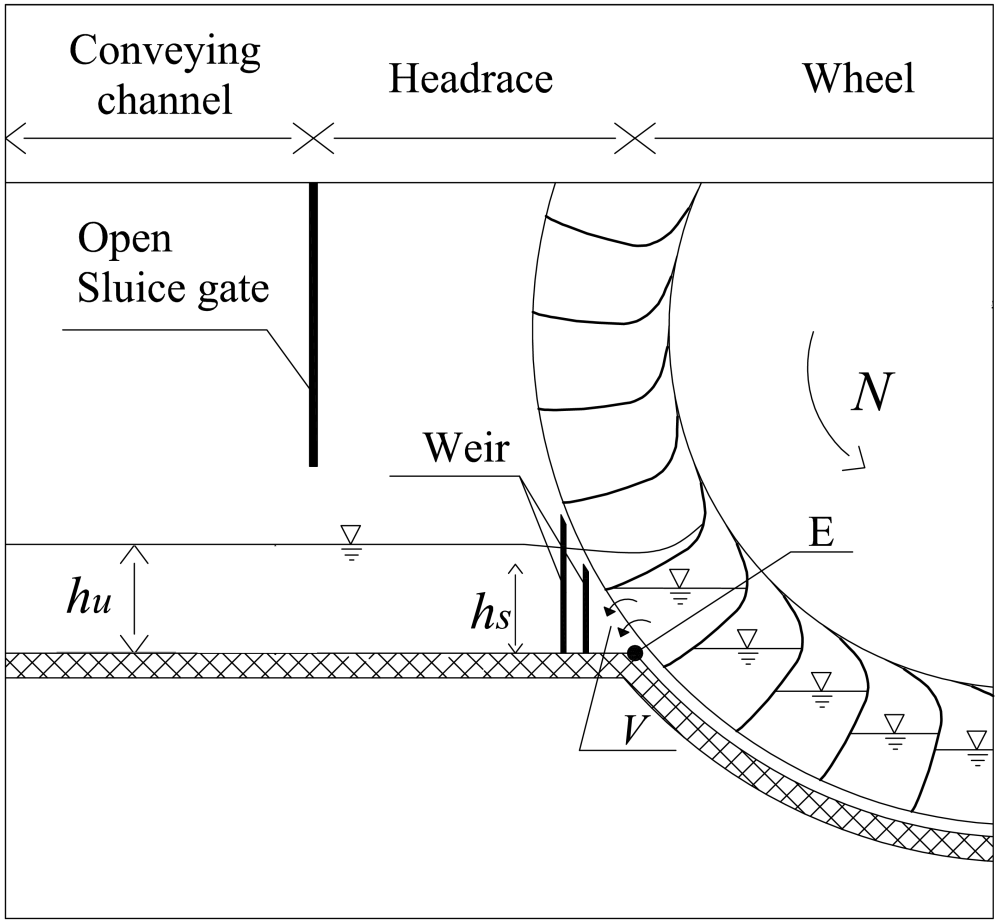

Fig. 5. The configuration with the sluice gate totally opened and the vertical overflow weirs just before the wheel. In the figure, h_s refers to the shortest weir.

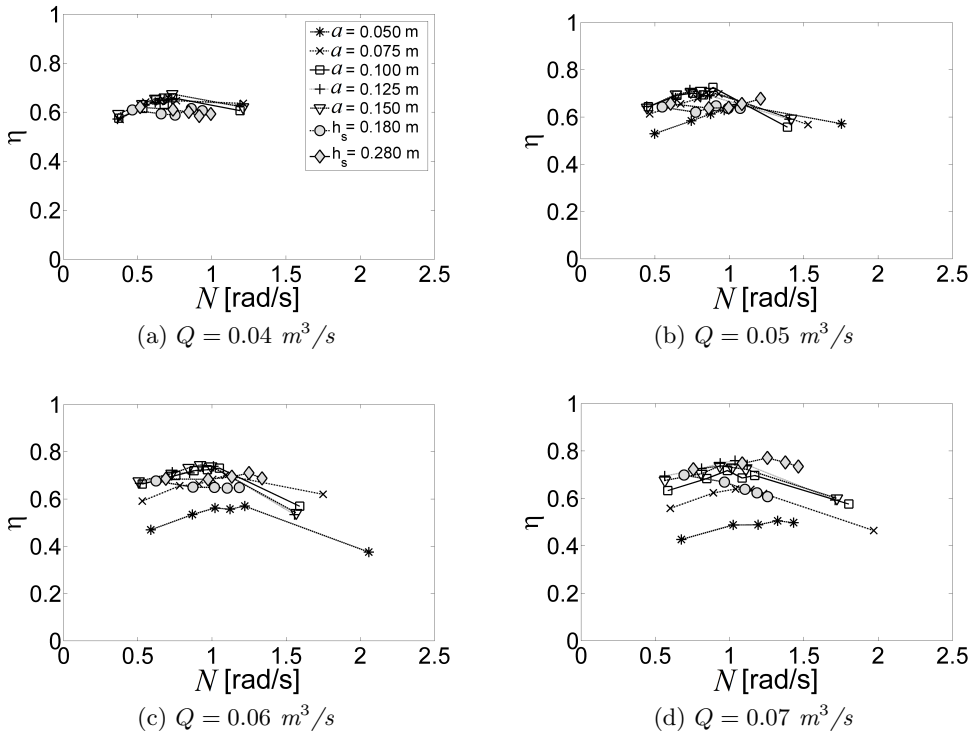

(a) $Q = 0.04\ m^3/s$ (b) $Q = 0.05\ m^3/s$

(c) $Q = 0.06\ m^3/s$ (d) $Q = 0.07\ m^3/s$

Fig. 6. Efficiency versus the wheel rotational speed for different inflow configurations and flow rates. The legend is shown in the figure at the top left corner. a is the sluice gate opening and h_s the weir height.

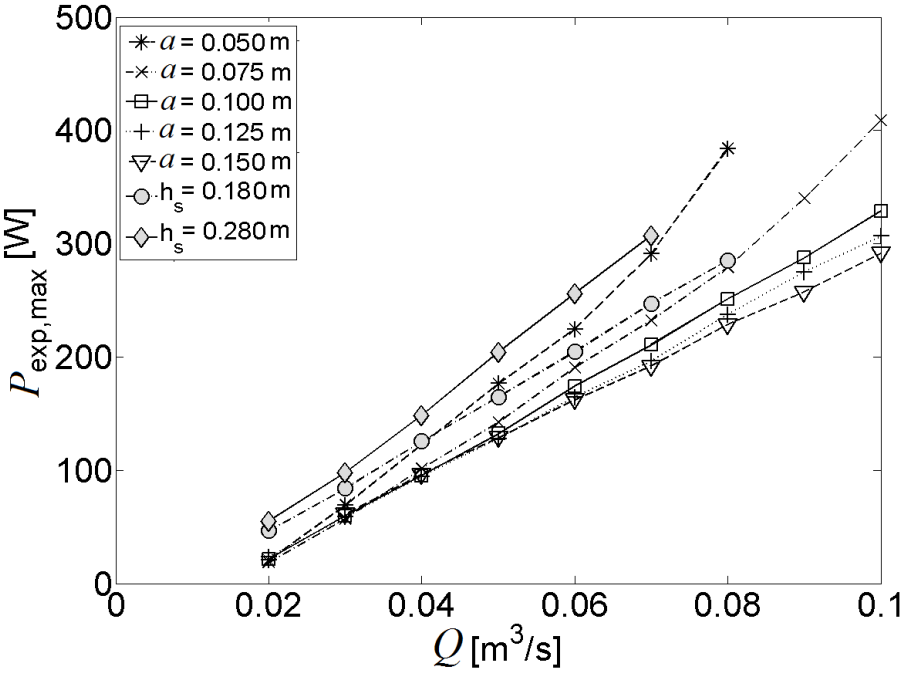

Fig. 7. Maximum experimental power output versus the flow rate. a is the sluice gate opening and h_s the weir height.

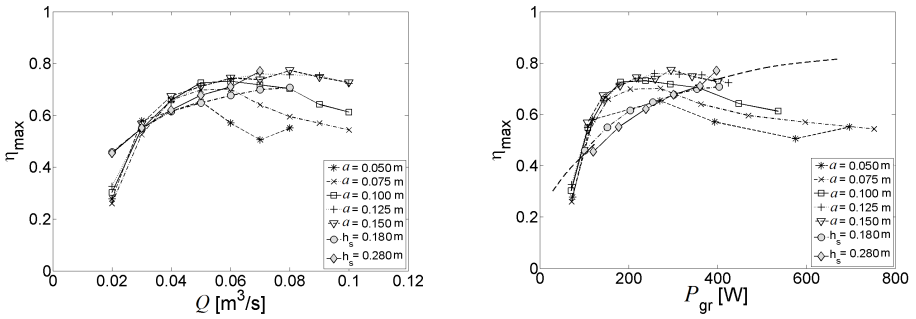

(a) (b)

Fig. 8. (a) Maximum efficiency versus the flow rate. (b) Maximum efficiency versus the power input. The dimension of the channel limited the exploitable flow rate to 0.08 m^3/s in some cases. The extrapolated trend for the weir configuration is represented with the dotted line. a is the sluice gate opening and h_s the weir height.

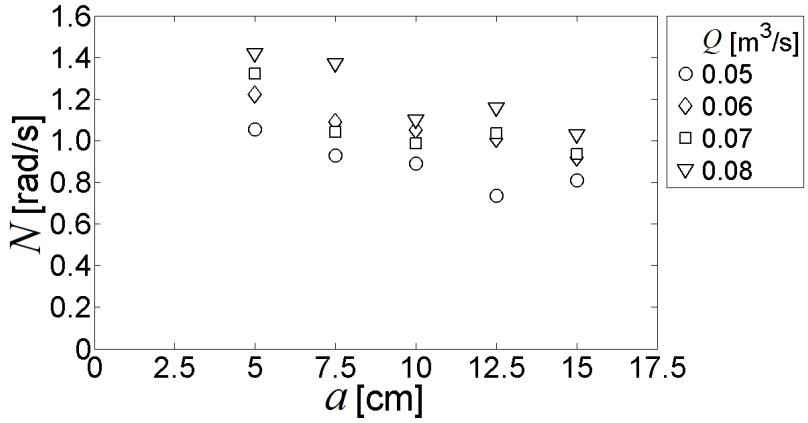

Fig. 9. Optimal rotational speeds of the wheel versus the sluice gate openings for some representative flow rates.

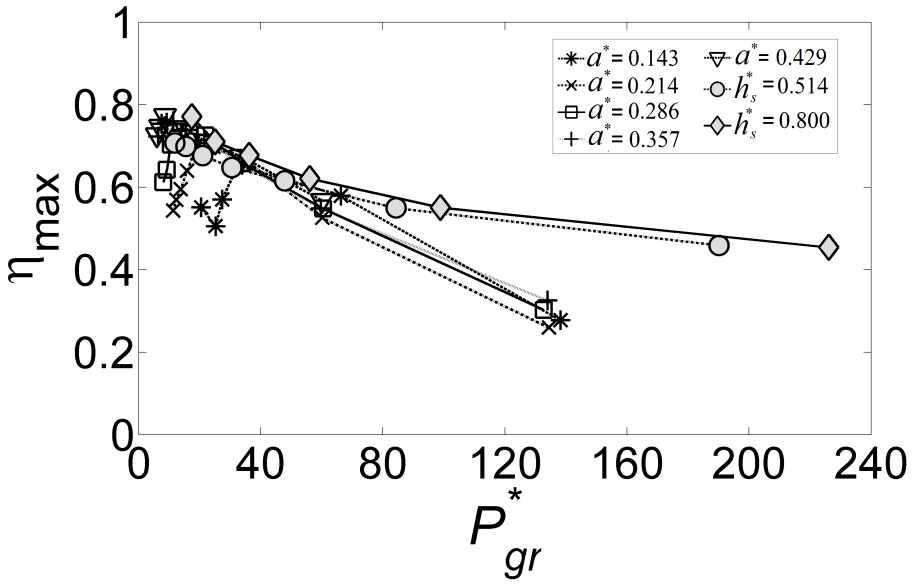

Fig. 10. Maximum efficiency versus the normalized power input. In the legend, the inflow configurations (a is the sluice gate opening and h_s is the height of the weir) are normalized to the geometric head difference $H_g = 0.35$ m, obtaining a^* and $h_s{}^*$.

Table 1. Normalized tangential speed of the wheel at the optimal efficiency for each inflow case and flow rate.

Inflow case (m)	Q (m^3/s)								
	0.02	0.03	0.04	0.05	0.06	0.07	0.08	0.09	0.10
a =0.05	0.06	0.21	-	0.34	0.36	0.35	0.36	-	-
a =0.075	0.10	0.18	0.27	0.34	0.38	0.34	0.42	0.41	0.34
a =0.1	0.10	0.22	0.29	0.35	0.40	0.36	0.39	0.35	0.36
a =0.125	0.12	0.19	0.29	0.29	0.39	0.40	0.44	0.37	0.38
a =0.15	-	0.22	0.29	0.32	0.36	0.36	0.40	0.37	0.45
h_s =0.18	0.099	0.24	0.29	0.30	0.21	0.23	0.25	-	-
h_s =0.28	0.13	0.18	0.16	0.37	0.38	0.39	-	-	-

Table 2. Filling ratio at the optimal efficiency for each inflow case and flow rate.

Inflow case (m)	Q (m^3/s)								
	0.02	0.03	0.04	0.05	0.06	0.07	0.08	0.09	0.10
a =0.05	0.72	0.31	-	0.28	0.29	0.31	0.33	-	-
a =0.075	0.45	0.38	0.33	0.32	0.32	0.39	0.34	0.37	0.47
a =0.1	0.46	0.32	0.32	0.33	0.33	0.42	0.43	0.51	0.53
a =0.125	0.40	0.37	0.32	0.40	0.35	0.40	0.41	0.53	0.55
a =0.15	-	0.32	0.32	0.36	0.38	0.44	0.46	0.55	0.49
h_s =0.18	0.40	0.24	0.27	0.32	0.57	0.59	0.62	-	-
h_s =0.28	0.29	0.30	0.45	0.24	0.28	0.33	-	-	-